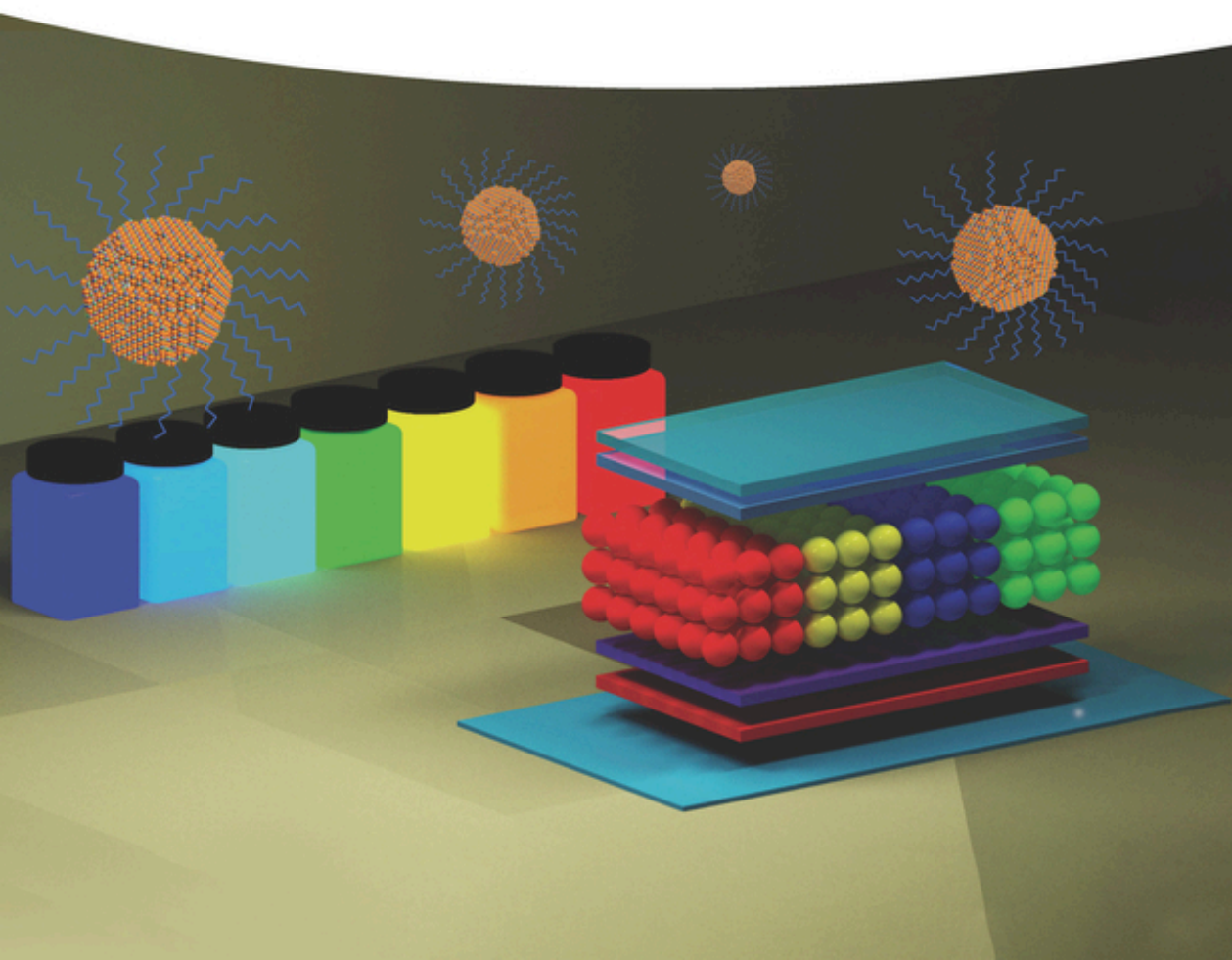


Hong Meng

Colloidal Quantum Dot Light Emitting Diodes

Materials and Devices



Colloidal Quantum Dot Light Emitting Diodes

Colloidal Quantum Dot Light Emitting Diodes

Materials and Devices

Hong Meng

Prof. Hong Meng

Peking University
Building G 306
Lishui Road, Nanshan District
Shenzhen
CH, 518055

Cover Image: © Prof. Hong Meng

■ All books published by **WILEY-VCH** are carefully produced. Nevertheless, authors, editors, and publisher do not warrant the information contained in these books, including this book, to be free of errors. Readers are advised to keep in mind that statements, data, illustrations, procedural details or other items may inadvertently be inaccurate.

Library of Congress Card No.: applied for

British Library Cataloguing-in-Publication Data

A catalogue record for this book is available from the British Library.

Bibliographic information published by the Deutsche Nationalbibliothek

The Deutsche Nationalbibliothek lists this publication in the Deutsche Nationalbibliografie; detailed bibliographic data are available on the Internet at <<http://dnb.d-nb.de>>.

© 2024 WILEY-VCH GmbH, Boschstr. 12, 69469 Weinheim, Germany

All rights reserved (including those of translation into other languages). No part of this book may be reproduced in any form – by photoprinting, microfilm, or any other means – nor transmitted or translated into a machine language without written permission from the publishers. Registered names, trademarks, etc. used in this book, even when not specifically marked as such, are not to be considered unprotected by law.

Print ISBN: 978-3-527-35327-9

ePDF ISBN: 978-3-527-84512-5

ePub ISBN: 978-3-527-84513-2

oBook ISBN: 978-3-527-84514-9

Typesetting Straive, Chennai, India

Contents

Preface *xi*

1	History and Introduction of QDs and QDLEDs	1
1.1	Preparation Route of Quantum Dots	3
1.2	Light-Emitting Characteristics of Quantum Dots	3
1.2.1	Particle Size and Emission Color	3
1.2.2	Quantum Dot Optical Property	4
1.2.2.1	Quantum Surface Effect	4
1.2.2.2	Quantum Size Effect	4
1.2.2.3	Quantum Confinement Effect	5
1.2.2.4	Quantum Tunnelling Effect	5
1.2.2.5	Quantum Optical Properties	6
1.2.3	Core–Shell Structure of QDs	8
1.2.4	Continuously Graded Core–Shell Structure of QDs (cg-QDs)	12
1.2.5	Typical QDs Materials	14
1.2.5.1	II–VI Semiconductor QDs	16
1.2.5.2	IV–VI Semiconductor QDs	17
1.2.5.3	II ₃ –V ₂ Semiconductor QDs	17
1.2.5.4	Ternary I–III–VI ₂ Chalcopyrite Semiconductor QDs	17
1.2.5.5	Single Element-Based Semiconductor QDs	17
1.3	Application of Quantum Dots on Display Devices	18
1.3.1	The Basic Structure of QDLED	18
1.3.2	Main Factors Affecting QDLED Light Emission	19
1.3.2.1	Auger Recombination (AR)	19
1.3.2.2	Fluorescence Resonance Energy Transfer	21
1.3.2.3	Surface Traps and Field Emission Burst	22
1.3.3	History of QDLED Development	22
1.4	Conclusion and Remarks	27
	References	28
2	Colloidal Semiconductor Quantum Dot LED Structure and Principles	33
2.1	Basic Concepts	33
2.1.1	Color Purity	33

2.1.2	Solution Processability	34
2.1.3	Stability	35
2.1.4	Surface States of Quantum Dots	36
2.1.5	Energy Levels and Energy Bands	36
2.1.6	Metals, Semiconductors, and Insulators	37
2.1.7	Electrons and Holes	38
2.1.8	Fermi Distribution Function and Fermi Energy Level	39
2.1.9	Schottky Barrier	39
2.1.10	Energy Level Alignment	40
2.2	Colloidal Quantum Dot Light-Emitting Devices	40
2.2.1	The Basic Structure of QDLED	41
2.2.2	The Working Principle of QDLED	43
2.2.3	Operating Parameters of QDLED	44
2.2.3.1	Turn-on Voltage	44
2.2.3.2	Luminous Brightness	44
2.2.3.3	Luminous Efficiency	44
2.2.3.4	Luminescence Color	45
2.2.3.5	Luminous Lifetime	45
2.2.3.6	QDLED Device Fabrication Process	48
	References	48
3	Synthesis and Characterization of Colloidal Semiconductor Quantum Dot Materials	51
3.1	Background	51
3.2	Synthesis and Post-processing of Colloidal Quantum Dots	53
3.2.1	Direct Heating Method and Hot Injection Synthesis Method	53
3.2.1.1	Hot-Injection Method	54
3.2.1.2	Direct Heating Method	55
3.2.2	Precursor Chemistry	56
3.2.3	Ligating and Non-ligating Solvents	56
3.2.4	Mechanism of Nucleation and Growth of Colloidal Quantum Dots	58
3.2.5	Size Distribution Focus and Size Distribution Scatter	59
3.2.6	Crystalline Species-Mediated Growth and Orientation of Nanocrystals Attachment Growth	60
3.2.7	Synthesis Methods and Band Gap Regulation Engineering of Nuclear-Shell Quantum Dots	61
3.2.7.1	Non-alloyed Core-Shell Quantum Dots	63
3.2.7.2	Alloy Core-Shell Quantum Dots	64
3.2.8	Surface Chemistry of Colloidal Quantum Dots	65
3.2.8.1	Covalent Bond Classification Method	65
3.2.8.2	Entropic Ligands	66
3.3	Material Characterization	66
3.3.1	Ultraviolet-Visible (UV-Vis) Absorption and Fluorescence Spectra	67
3.3.2	Nuclear Magnetic Resonance Spectroscopy	69
3.3.3	Fourier Transform Infrared Spectroscopy (FTIR)	71

3.3.4	X-Ray Photoelectron Spectroscopy (XPS)	74
3.3.5	Transmission Electron Microscopy	76
3.3.6	Small-Angle X-Ray Scattering and Wide-Angle X-Ray Scattering	76
3.3.7	X-Ray Diffractometer	77
3.3.8	X-Ray Absorption Fine Structure Spectra	78
3.3.9	Measurement of Fluorescence Quantum Yield	79
3.4	Conclusion and Outlook	79
	References	81
4	Red Quantum Dot Light-Emitting Diodes	87
4.1	Background	87
4.2	Red Light Quantum Dot Materials	88
4.2.1	Materials	89
4.2.2	Quantum Dot Structure Design and Optimization	90
4.2.3	Surface Ligands	91
4.2.4	Core-Shell Structure	94
4.2.5	Alloy Core-Shell Structure	96
4.3	Red QDLED Devices	97
4.3.1	Red QDLED Device Architecture Development	97
4.3.2	Common Device Structures	99
4.4	Conclusion and Outlook	102
	References	104
5	Green Quantum Dot LED Materials and Devices	111
5.1	Background	111
5.2	Commonly Used Luminescent Layer Materials in Green QDLEDs	120
5.2.1	Discrete Core/Shell Quantum Dots	120
5.2.2	Alloyed Core/Shell Quantum Dots	121
5.2.3	Core/Multilayer Shell Quantum Dots	121
5.3	Development of Device Structures for Green QDLEDs	122
5.4	Factors Affecting the Performance of Green QDLEDs	125
5.4.1	QD Ligand Effect	126
5.4.2	QD Core/Shell Structure	129
5.4.3	Optimization of the Device Structure	130
5.4.4	Other Strategies to Improve Device Performance	132
5.5	Summary and Outlook	134
	References	135
6	Blue Quantum Dot Light-Emitting Diodes	141
6.1	Introduction	141
6.2	Blue Quantum Dot Luminescent Materials	143
6.2.1	Blue Quantum Dots Containing Cadmium	145
6.2.2	Cadmium-Free Quantum Dots	149
6.2.2.1	Quantum Dots Based on InP	149
6.2.2.2	Quantum Dots Based on ZnSe	151

6.2.2.3	Quantum Dots Based on Cu	153
6.2.2.4	Quantum Dots Based on AlSb	155
6.3	Optimization of Charge Transport Layer (CTL)	155
6.3.1	Hole Transport Layer	156
6.3.2	Electron Transport Layer	161
6.4	Device Structure	164
6.5	Summary	166
	References	168
7	Near-Infrared Quantum Dots (NIR QDs)	173
7.1	Introduction of Near-Infrared Quantum Dots	173
7.2	Near-Infrared Quantum Dot Materials	174
7.2.1	Chalcogenide Lead Quantum Dots	176
7.2.2	Chalcogenide Cadmium Quantum Dots	177
7.2.3	Silicon Quantum Dots	178
7.3	Optimization of Near-Infrared Quantum Dot Materials	179
7.3.1	Regulation of Near-Infrared Quantum Dots by Ligand Engineering	179
7.3.2	Control of Near-Infrared Quantum Dots by Core/Shell Structure	180
7.3.3	Quantum Dots in the Matrix	181
7.4	Summary and Prospect	182
	References	183
8	White QDLED	187
8.1	Generation of White Light	187
8.2	Quantum Dots for White LEDs	188
8.2.1	Yellow–Blue Composite White Light Quantum Dots	189
8.2.1.1	Cadmium-Containing Yellow Light Quantum Dots	189
8.2.1.2	Cadmium-Free Yellow Light Quantum Dots	189
8.2.2	Three-Base Color Quantum Dot Composite	193
8.2.3	Quantum Dots with Direct White Light Emission	197
8.3	Summary Outlook	200
	References	203
9	Non-Cadmium Quantum Dot Light-Emitting Materials and Devices	207
9.1	Introduction	207
9.2	Quantum Dots and QDLED	208
9.2.1	InP	208
9.2.2	ZnSe	215
9.2.3	I-III-VI	218
9.3	Methods for Optimizing QDLED Performance	222
9.3.1	Ligand Engineering	223
9.3.2	Shell Engineering	224
9.3.3	QDLED Device Structure Optimization	225
9.4	Summary and Outlook	227
	References	230

10	AC-Driven Quantum Dot Light-Emitting Diodes	235
10.1	Principle of Luminescence of DC and AC-Driven QDLEDs	236
10.2	Mechanism of Double-Emission Tandem Structure of AC QDLEDs	239
10.2.1	Field-Generated AC QDLEDs	240
10.2.2	Half-Field to Half-Injection AC QDLEDs	242
10.2.3	AC/DC Dual Drive Mode QDLEDs	244
10.3	Optimization Strategies for AC QDLEDs	245
10.3.1	Optimization of the Field-Induced AC QDLED	247
10.3.1.1	Dielectric Layer Optimization	248
10.3.1.2	Quantum Dot Layer Optimization	250
10.3.2	Optimization of Half-Field-Driven Half-Injected AC QDLEDs	251
10.3.2.1	Charge Generation Layer Optimization	254
10.3.2.2	Tandem Structure	254
10.3.2.3	AC/DC Dual Drive Mode QDLED Optimization	255
10.3.3	Conclusion and Future Direction of AC-QDLED	256
	References	257
11	Stability Study and Decay Mechanism of Quantum Dot Light-Emitting Diodes	259
11.1	Quantum Dot Light-Emitting Diode Stability Research Status	259
11.2	Factors Affecting the Stability of Quantum Dot Light-Emitting Diodes	261
11.2.1	Quantum Dot Light-Emitting Layer	261
11.2.2	Hole Transport Layer	263
11.2.3	Electronic Transport Layer	265
11.2.4	Other Functional Layers	267
11.3	Quantum Dot Light-Emitting Diode Efficiency Decay Mechanism	268
11.4	Aging Mechanisms of QDLEDs	271
11.4.1	Positive Aging	272
11.4.2	Negative Aging	273
11.4.3	Electron Transport Layer	274
11.4.4	Hole Transport Layer	275
11.4.5	QDs Layer	276
11.5	Characterization Technologies for QDLEDs	278
11.5.1	Transient Electroluminescence	279
11.5.2	Electro-Absorption (EA) Spectroscopy	281
11.5.3	In-Situ EL-PL Measurement	282
11.5.4	Differential Absorption Spectroscopy	283
11.5.5	Displacement Current Measurement DCM Technology	285
11.6	Outlook	286
	References	287
12	Electron/Hole Injection and Transport Materials in Quantum Dot Light-Emitting Diodes	291
12.1	Introduction	291
12.2	Charge-Transport Mechanisms	292

12.3	Electron Transport Materials (ETMs) for QDLED	293
12.3.1	Metal-Doped ETMs	293
12.3.2	Metal Salt-Doped ETMs	296
12.3.3	Design of Composite Materials ETMs	296
12.3.4	Polymer-Modified ETMs	296
12.3.5	Inorganic Organic Hybrid ETMs	296
12.3.6	Double-Stacked ETMs	297
12.4	Electron Injection Materials for QDLED	299
12.5	Hole Transport Materials for QDLED	301
12.5.1	Doping of HTMs	305
12.5.2	Compositions of HTMS	309
12.5.3	New HTM Materials for QDLED	311
12.6	Hole Injection Materials for QDLED	315
12.7	Summary and Outlook	321
	References	322
13	Quantum Dot Industrial Development and Patent Layout	327
13.1	Introduction	327
13.2	Patent Layout	330
13.2.1	Nanosys	330
13.2.2	SAMSUNG	332
13.2.3	Nanoco	335
13.2.4	Najing Tech	338
13.2.5	CSOT	344
13.2.6	BOE	347
13.2.7	TCL	351
13.3	Summary and Outlook	355
	References	355
14	Patterning Techniques for Quantum Dot Light-Emitting Diodes (QDLED)	361
14.1	Introduction	361
14.2	Photolithography	361
14.3	Micro-Contact Transfer	363
14.4	Inkjet Printing	366
14.5	Other Patterning Techniques	368
14.6	Conclusion	369
	References	370
	Index	373

Preface

Light has played a significant role in human life since the beginning of civilization, from the discovery of fire to the invention of electric light. As technology has advanced, so has the need for more efficient, cost-effective, and environmentally friendly lighting solutions. The advent of quantum dot light-emitting diodes (QDLEDs) is a significant step forward in the development of new-generation display and lighting technologies. QDLEDs have shown tremendous potential in various fields, including flat-panel displays and solid-state lighting.

This book aims to provide an in-depth understanding of the recent developments in colloidal quantum dot light-emitting materials and devices. It comprises 14 chapters that discuss key materials and optimization schemes for QDLEDs, exploring the relationship between material synthesis and device performance. The first chapter provides a brief overview of the history and development of quantum dots and QDLEDs, while the second chapter introduces the structure and operating principles of QDLEDs. Chapters 3–9 review the latest research results in red, green, blue, near-infrared, white, and cadmium-free quantum dot light-emitting materials and devices. Chapter 10 discusses the luminescence principles of AC-driven QDLEDs, and Chapter 11 delves into the stability study and decay mechanism of QDLEDs. Chapter 12 covers electron/hole injection and transport materials in QDLEDs, and Chapter 13 summarizes the industrialization development and patent layout of quantum dots, while Chapter 14 illustrates the patterning and printing technology in QDLED development.

The author of this book has extensively researched the latest progress and results in academia and industry, citing relevant contents, diagrams, and data in the references. This book is a collaborative effort, with contributions from researchers at various levels, including PhD and MS students, who have made significant contributions to the formation and drafting of the book content in Chinese. The publication of this book would not have been possible without the support and help of the relevant staff of the publisher and the assistance of ChatGPT during the editing and finalization of the book in English.

The author of this book would like to express his sincere gratitude to everyone who has contributed to the creation and publication of this book. The team of authors is thankful to their students, postdocs, research assistants, and staff for their hard work and dedication in researching and writing this first-edition book in Chinese.

They also appreciate the editors, translators, proofreaders, and designers who helped to bring the book to life in multiple languages and formats. Lastly, the authors extend their heartfelt thanks to their families, colleagues, and friends for their unwavering support and encouragement throughout this project.

This book is a culmination of the authors' efforts to share their knowledge and expertise on colloidal quantum dot light-emitting materials and devices with readers. It is hoped that this book will serve as a useful reference for researchers, scientists, engineers, students, and anyone interested in the development and application of QDLEDs. The authors believe that the contents of this book will help promote the research and development of QDLEDs and contribute to the progress of the lighting and display industries.

May 2023

Hong Meng
School of Advanced Materials
Peking University Shenzhen Graduate School
Peking University
Shenzhen
518055 China
E-mail: menghong@pku.edu.cn

1

History and Introduction of QDs and QDLEDs

Semiconductor nanocrystals (NCs) are the most widely studied of the nanoscale semiconductors. In early 1981, Alexei Ekimov and Alexander Efros, working at the S.I. Vavilov State Optical Institute and A.F. Ioffe Institute, Russia, discovered nanocrystalline, semiconducting quantum dots (QDs) in a glass matrix and conducted pioneering studies of their electronic and optical properties. Simultaneously, in 1985, Louis Brus at Bell Laboratories in Murray Hill, NJ, discovered colloidal semiconductor NCs (QDs), for which he shared the 2008 Kavli Prize in Nanotechnology. Over the years, QDs have been established as a new type of semiconductor nanocrystalline material whose size is smaller than or close to the excitonic Bohr radius of its bulk material. Common semiconductor materials include Si, Ge, compounds of group II–VI (e.g. CdSe), and compounds of group III–V (e.g. indium phosphide [InP]). When the size of these bulk semiconductor materials is larger than their exciton Bohr radii, electrons and holes are able to move freely and independently in the bulk materials. However, when the size of QDs is smaller than their own exciton Bohr radius, after being excited by light, an electron in the valence band will leap to the conduction band, leaving a hole in the valence band, and the electron and hole form an exciton due to Coulomb effect, which is confined in a space smaller than the exciton Bohr radius, and the electron and hole will be quantized, which is called the “quantum size effect” of nanomaterials. This quantum size effect allows QDs to have discrete energy levels, thus giving them unique physicochemical properties [1]. Colloidal semiconductor NCs have size-dependent particle properties, while their surface ligands make them solution-processable, which gives them a “particle-solution” duality.

Figure 1.1a shows the energy level diagrams of molecular, QD, and bulk semiconductor materials. The molecular orbital energy level diagram is composed of the highest occupied molecular orbital (HOMO) and the lowest unoccupied molecular orbital (LUMO), while the energy level diagram of QDs consists of some discrete energy levels, and the bulk semiconductor material consists of conduction and valence bands. Figure 1.1b illustrates the spatial extent of the confined domains of electrons and holes and the respective energy as a function of the density of electronic states for bulk semiconductor materials, two-dimensional

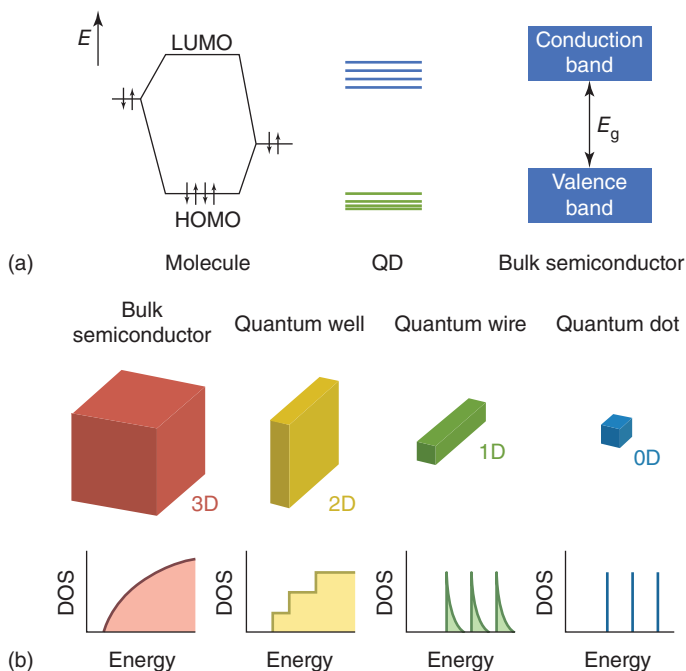


Figure 1.1 (a) Schematic diagram of energy levels of molecular, quantum dot, and bulk semiconductor materials; (b) spatial extent of the confined domain of electrons and holes and the respective energy as a function of the density of electronic states for bulk semiconductor materials, two-dimensional quantum sheets, one-dimensional quantum wires, and zero-dimensional quantum dots depending on the material size.

quantum sheets, one-dimensional quantum wires, and zero-dimensional QDs, depending on the size of the material. For a bulk semiconductor material, the dimensions in all three dimensions are larger than its own Bohr exciton radius, and electrons and holes are free to move independently in all three dimensions; while for a two-dimensional quantum sheet, the dimensions in two dimensions are larger than its own Bohr exciton radius, and electrons and holes are free to move independently in two dimensions; and for a one-dimensional quantum wire, the dimensions in one dimension are larger than its own Bohr exciton radius, while for a one-dimensional quantum wire, whose dimension in one dimension is larger than its own exciton radius, electrons and holes are free to move independently in one dimension; and for a zero-dimensional QD, whose dimension in all three dimensions is smaller than its own exciton radius, electrons and holes are restricted from moving freely and independently in all dimensions. In general, QD is a collective term for a two-dimensional quantum sheet, a one-dimensional quantum wire, and a zero-dimensional QD.

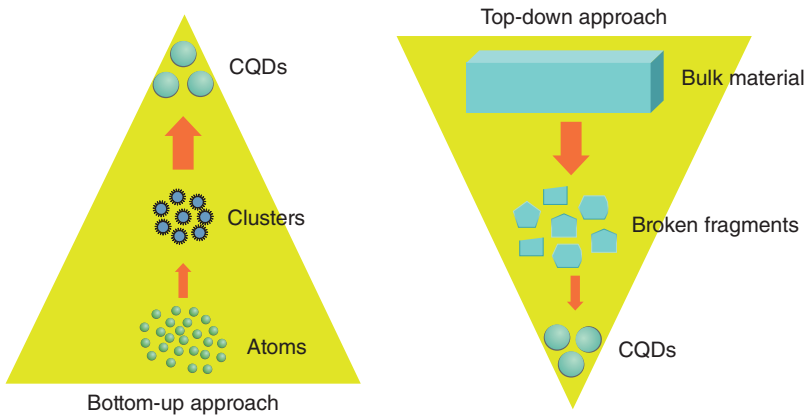


Figure 1.2 Preparation pathways for quantum dots: the “top-down” method and the “bottom-up” method.

1.1 Preparation Route of Quantum Dots

There are two completely different ways to prepare QDs, namely the “top-down method” and the “bottom-up method”, as shown in Figure 1.2. The top-down method is to prepare QDs by reducing the dimensionality and size of the bulk semiconductor material; the bottom-up method is to combine atoms or molecules into QDs by chemical synthesis. The former approach is limited by the ultra-fine processing technology, which cannot produce QDs below 10 nm at present, and the morphological regulation of QDs is also limited to some extent. The latter is mainly achieved through colloidal chemical synthesis, which can produce colloidal QDs of different sizes and shapes.

1.2 Light-Emitting Characteristics of Quantum Dots

1.2.1 Particle Size and Emission Color

QDs are semiconductor particles having a few nanometers in size, their optical and electronic properties are quite different from those of larger particles as a result of quantum mechanics. When the QDs are illuminated by UV light, an electron in the QD can be excited from the transition of an electron valence band to the conduction band. The excited electron can drop back into the valence band releasing its energy as light. The color of that light depends on the energy difference between the conduction band and the valence band. The QD absorption and emission features correspond to transitions between discrete quantum mechanically allowed energy levels in the box, which are reminiscent of atomic spectra.

1.2.2 Quantum Dot Optical Property

The QDs are defined as the semiconductor NCs with the quantum confinement. Thus, the semiconductor nanoparticles with dimensions QDs have the following features:

1.2.2.1 Quantum Surface Effect

The surface effect refers to the fact that as the particle size of QDs decreases, most of the atoms are located on the surface of QDs, and the specific surface area of quantum dots increases with decreasing particle size. Due to the large specific surface area of QDs (nanoparticles), the increase in the number of atoms in the surface phase leads to the lack of coordination, unsaturated bonds, and suspension bonds of surface atoms. This makes these surface atoms highly reactive, extremely unstable, and easily bonded with other atoms. This surface effect will cause the large surface energy and high activity of nanoparticles. The activity of surface atoms not only causes changes in the surface atomic transport and structural type of nanoparticles but also causes changes in the surface electron spin conformation and electronic energy spectrum. This feature offers a route to manipulate QD interactions with their environment. QDs can be tethered to proteins, antibodies, or other biologic species and used as optically addressable bio-labels. On the other hand, passivation of QD surface can improve the QD stability and increase the photoluminescent quantum efficiency. Surface defects lead to trapped electrons or holes, which in turn affect the luminescent properties of QDs and cause nonlinear optical effects. Metallic materials show various characteristic colors through light reflection. Due to the surface effect and size effect, the light reflection coefficient of nanoparticles decreases significantly, usually less than 1%, so nanoparticles are generally black in color, and the smaller the particle size, the darker the color, i.e. the stronger the light absorption ability of nanoparticles, showing a broadband strong absorption spectrum. Surface effect or ligand modification offers an additional tool for manipulating energy levels and electronic and optical properties.

1.2.2.2 Quantum Size Effect

Quantum size effect refers to the phenomenon that the electron energy levels near the Fermi energy level change from quasi-continuous to discrete energy levels, that is, when the particle size drops to a certain value, the energy level splits or energy gap widens, in other words, the energy spectrum becomes discrete, and as a result, the bandgap becomes size-dependent. When the change in energy level is greater than the change in thermal, optical, and electromagnetic energy, it leads to the magnetic, optical, acoustic, thermal, electrical and superconducting properties of nanoparticles being significantly different from those of conventional materials. This feature of QDs is that the energy gap changes with the increase in the grain size, the larger the grain size, the smaller the energy gap, and *vice versa*, the larger the energy gap. That is, the smaller the QD, the shorter the wavelength of light (blueshift), and the larger the QD, the longer the wavelength of light (redshift). According to the size effect of QDs, we can use the method of changing the size of the grain to regulate

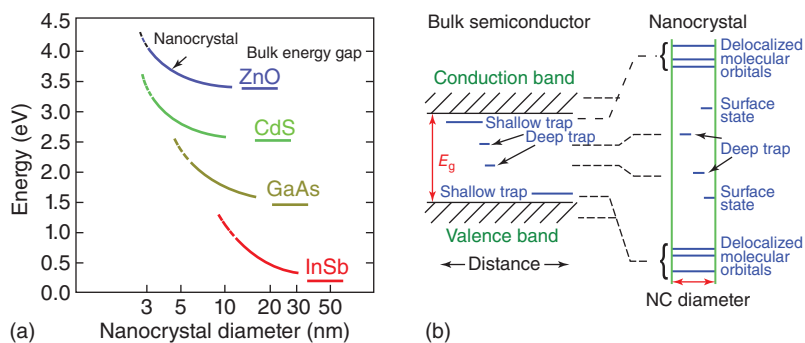


Figure 1.3 Theoretical ideas from the early 1980s. (a) Calculated size-dependent shift of the lowest exciton levels in strong confinement (b) Spatial electronic state correlation diagram for bulk semiconductors and NCs. The bulk valence and conduction bands, together with shallow trap states, evolve into the NC molecular orbitals. Deeply localized defect states in the bulk have essentially the same energy as those in the NC. New localized surface states exist in the NC. Source: Efros and Brus [2]/American Chemical society.

the tuning of the light spectrum of the material and no longer need to change the chemical composition of QDs.

1.2.2.3 Quantum Confinement Effect

Quantum confinement can be observed once the diameter of a material is of the same magnitude as the de Broglie wavelength of the electron wave function. When the QD size of the particle reaches the nanometer scale, the electronic energy level near the Fermi energy level splits from the continuum to the discrete energy level, and their electronic and optical properties deviate substantially from those of bulk materials (Figure 1.3). For semiconductor materials, the size of the bandgap can be adjusted by changing the scale of the particles, thus changing the reliance on certain very costly semiconductor materials (Figure 1.4). Quantum confinement effects in QDs can also result in fluorescence intermittency, called “blinking” [4].

1.2.2.4 Quantum Tunnelling Effect

Quantum tunneling effect is one of the fundamental quantum phenomena, i.e. when the total energy of a microscopic particle is less than the height of the potential barrier, considering the motion of a particle encountering a potential barrier above the energy of the particle, the particle is still able to cross this barrier, which indicates that on the other side of the barrier, the particle has a certain probability that the particle penetrates the potential barrier. For QDs, electron movement in the nanoscale space, the carrier transport process will have obvious electronic fluctuations, the emergence of quantum tunneling effect, and the energy level of the electron is discrete [5]. To achieve the quantum effect, it requires the formation of nano-conducting domain in a few μm to tens of μm tiny area. When the voltage is low, the electrons are confined to the nanoscale range of motion, and increasing the voltage can make the electrons cross the nanopotential barrier to form a sea of Fermi electrons, making the system conductive. The

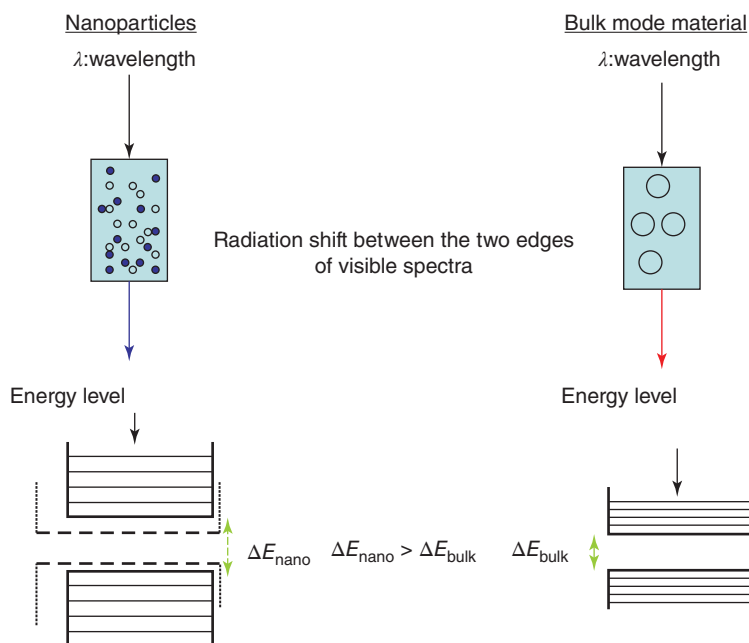


Figure 1.4 QDs Confinement effect: As the size of the particles decreases, the electrons and electron holes come closer, and the energy required to activate them increases, which ultimately results in a blueshift in light emission. Source: Adapted from Kang and Min [3].

quantum tunneling effect occurs when electrons cross the quantum barrier from one quantum well into another quantum well, and this insulating to conducting critical effect is a characteristic of the QDs in a nano-ordered array system. Most QD solids exhibit complex charge-carrier interactions between carrier confinement, interfacial properties, and quantum tunneling effects in the nature of electronic coupling [6].

1.2.2.5 Quantum Optical Properties

Owing to the above-mentioned effects of QDs, the QD absorption and emission features correspond to transitions between discrete quantum mechanically allowed energy levels in the box, which are reminiscent of atomic spectra. QDs have intermediate properties between bulk semiconductors and discrete atoms or molecules. Their optoelectronic properties change as a function of both size and shape. Larger QDs of 5–6 nm diameter emit longer wavelengths, with colors such as orange, or red. Smaller QDs (2–3 nm) emit shorter wavelengths, yielding colors like blue and green. Whereas, the specific colors vary depending on the exact composition of the QD. It turns out that QDs have broad absorption spectra, meaning that they can be excited across a pretty expansive range of light wavelengths. Figure 1.5 shows the emission color of QDs dependent on their respective sizes.

Recent studies have also shown that the shape of the QD may play a role in the band-level energy of the QD, thus affecting the frequency of fluorescence emission

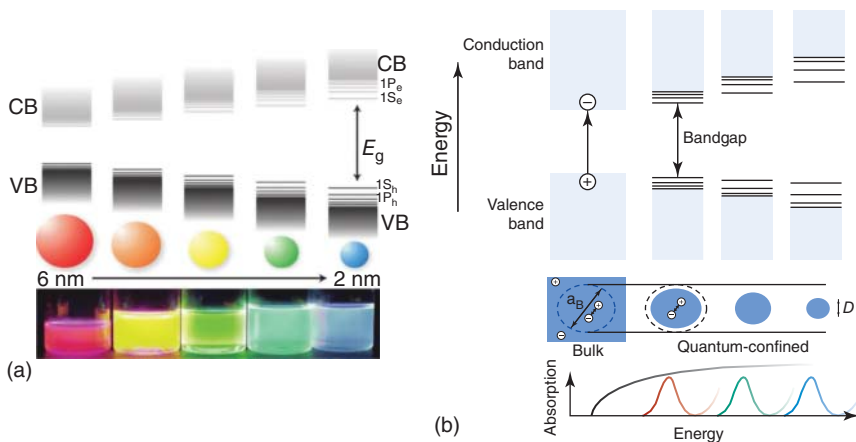


Figure 1.5 (a) Schematic representation of the quantum confinement effect on the energy level structure of a semiconductor material. The lower panel shows colloidal suspensions of CdSe NCs of different sizes under UV excitation. Source: Donegá [7]/Royal Society of Chemistry.; (b) Quantum confinement, leading to size-dependent optical and electrical properties that are distinct from those of parental bulk solids, occurs when the spatial extent of electronic wave functions is smaller than the Bohr exciton diameter. Source: García de Arquer et al. [8]/American Association for the Advancement of Science.

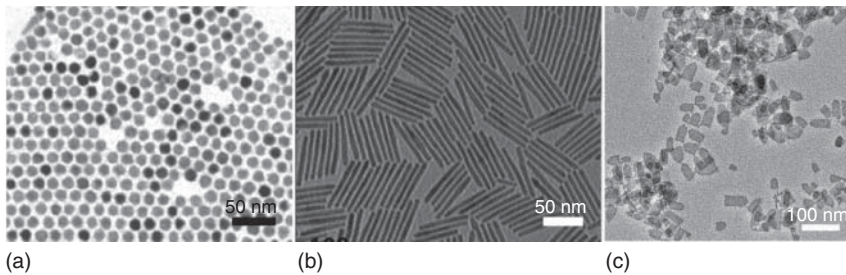


Figure 1.6 Pictures of quantum dots with various sizes and morphologies taken with transmission electron microscopy (a) quantum dots, (b) quantum rods, and (c) quantum sheets.

or absorption. The luminescence characteristics of QDs are closely related to their size and shape, the presence or absence of core–shell structure, and their surface chemistry. QDs of various sizes, morphologies, and core–shell structures can be synthesized by colloidal chemistry, as shown in the transmission electron microscope image in Figure 1.6.

The ligand type and ligand concentration on the surface of colloidal QDs also have an effect on their luminescence properties. For example, Peng et al. observed a shift of several nanometers in the peak position of the fluorescence emission peak of CdSe/CdS core–shell structured QDs ligated by fatty acid cadmium salt surface after ligand exchange treatment by aliphatic amines (Figure 1.7). The QDLED luminescence performance indexes such as external quantum yield and lifetime of CdSe/CdS core–shell QDs with different surface ligands are even more different when prepared

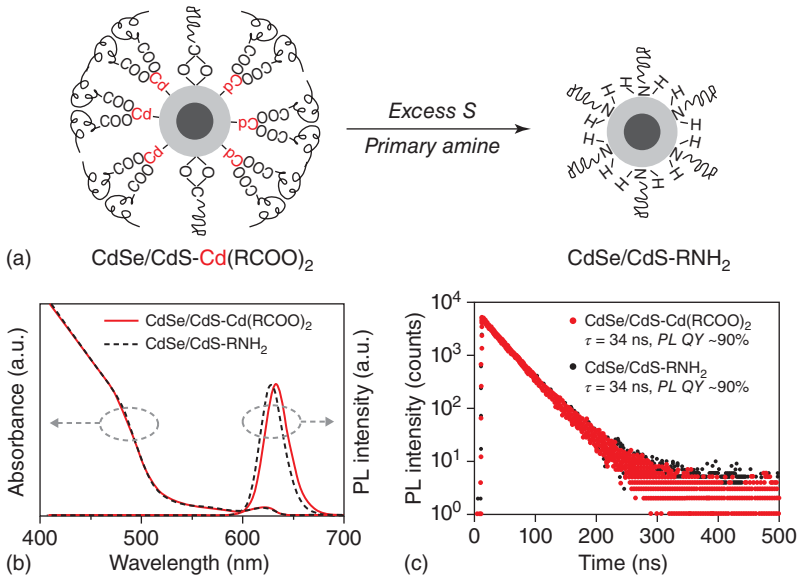


Figure 1.7 Photoluminescence and electroluminescence properties of CdSe/CdS-Cd(RCOO)₂ and CdSe/CdS-RNH₂ quantum dots. Schematic diagram of CdSe/CdS quantum dots with fatty acid cadmium surface ligands (and also a small amount of negatively charged carboxylates) undergoing ligand exchange to generate CdSe/CdS quantum dots with aliphatic amines. (b) Absorption and steady-state photoluminescence spectra. (c) Time-resolved photoluminescence spectrum with single-exponential decay lifetime (τ) and quantum yield (QY). Source: Pu et al. [9]/CC BY 4.0/Public Domain.

into QDLED devices [9]. Therefore, we should pay special attention to the surface chemical state when studying the luminescence properties of QDs.

The effect of crystal structure can also affect the emission color. Table 1.1 illustrates common bulk semiconductor physical properties. The crystal lattice of a QD semiconductor has an effect on the electronic wave function. As a result, QDs have a specific energy spectrum equal to the bandgap and a specific density of electronic states outside the crystal. Compared to conventional fluorophores, QDs have unique optical and electronic properties. Examples include high quantum yields and molar extinction coefficients, large effective Stokes shifts, broad excitation spectra, narrow emission spectra, a high resistance to reactive oxygen species, protection against material degradation, and nearly impervious to photobleaching.

In highly monodisperse colloidal QD samples, due to the quantum size effect, electrons and holes are subjected to quantum confinement effect, atomic-like structure of electronic states of QDs leads to the formation of discrete energy levels of narrow full-width at half maximum (FWHM) width of 20–80 meV at room temperature and symmetrical fluorescence emission peaks [10] (Figure 1.8).

1.2.3 Core–Shell Structure of QDs

For most core QDs, due to their low PLQYs and poor stabilities, they tend to exhibit a broad red-shifted emission, owing to the surface defects. The issues can be

Table 1.1 Common bulk semiconductor physical parameters.

Material name	Crystal structure type (300 K)	Category	E_{gap} (eV)	Lattice parameters (Å)	Density (g cm^{-3})
ZnS	Sphalerite	II–VI	3.61	5.41	4.09
ZnSe	Sphalerite	II–VI	2.69	5.67	5.27
ZnTe	Sphalerite	II–VI	2.39	6.10	5.64
CdS	Wurtzite	II–VI	2.49	4.14/6.71	4.82
CdSe	Wurtzite	II–VI	1.74	4.3/7.01	5.81
CdTe	Sphalerite	II–VI	1.43	6.48	5.87
InP	Sphalerite	III–V	1.35	5.87	4.79
GaAs	Sphalerite	III–V	1.42	5.65	5.32
PbS	Rock salt	IV–VI	0.41	5.94	7.60
PbSe	Rock salt	IV–VI	0.28	6.12	8.26
PbTe	Rock salt	IV–VI	0.31	6.46	8.22

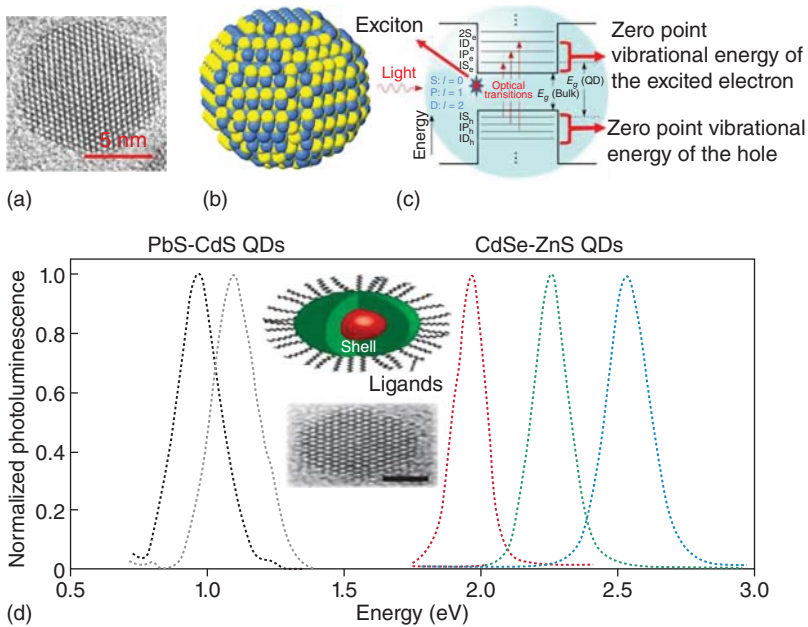


Figure 1.8 (a) TEM image of CdSe nanocrystal; (b) nanocrystal atomic structure; (c) energy level discreteness of the excited electron and the hole in an exciton entity. (d) PL spectra of CdSe–ZnS and PbS–CdS core/shell colloidal QDs. Source: Efros and Brus [2]/American Chemical Society.

addressed to improve efficiency and brightness of semiconductor NCs by growing shells of another higher-bandgap semiconducting material around them, resulting in core-shell QDs. The improvement is due to the reduced access of electrons and holes to non-radiative surface recombination pathways, and in other cases, due to the reduced Auger recombination (AR). Core-shell QDs (core@shell QDs) hold the promise of being emissive components through the precise control of shade and an improved color-rendering index. They exhibit improved optical properties over pure core-only QDs due to the growth of the shell around the QD core, which improves stability and photoluminescence efficiency. A fundamental feature of QDs is the tunability of their emission color through precise control of their size and composition, giving access to UV, visible, and near-infrared wavelengths. Continuing improvements in engineering core-shell QD structures, where a 1–10 nm binary, ternary, or alloyed semiconductor core particle is surrounded by a shell composed of one or more semiconductors of a wider bandgap, have resulted in materials with fluorescence quantum yields that approach unity, narrow symmetric spectral line shapes, and remarkable stabilities, as shown in Figure 1.9, for CdSe/ZnS QDs [11], CdSe/CdS quantum rods [12], CdSe quantum sheets [13]. Interestingly, the fluorescence emission peaks of QDs and quantum rods have a large Stokes shift with the peak position of their first exciton absorption peaks, while the fluorescence emission peaks of quantum sheets have almost no Stokes shift with the peak position of their first exciton absorption peaks. In addition, in terms of fluorescence lifetime, the fluorescence lifetime of rare-earth luminescent materials is at millisecond or microsecond level, while the fluorescence lifetime of QDs is usually in the range of milliseconds [14–16]. While the fluorescence lifetime of QDs is usually below 100 ns [17–19]. It has been found that the fluorescence emission of single QDs has severe blinking behavior, ranging from a few milliseconds to a few minutes, which is mainly due to the non-radiative compounding process caused by the “surface defects” of QDs [20–22].

Although the PL of II–VI QDs can be bright and stable under a reasonable range of excitation light intensities, core-shell QDs universally showed significant “blinking” under the high fluxes used in single QD fluorescence spectroscopy, whereby the PL of single QDs turns “on” and “off” under continuous excitation. This single QD “blinking” not only limits the use of QDs as single photon sources but also

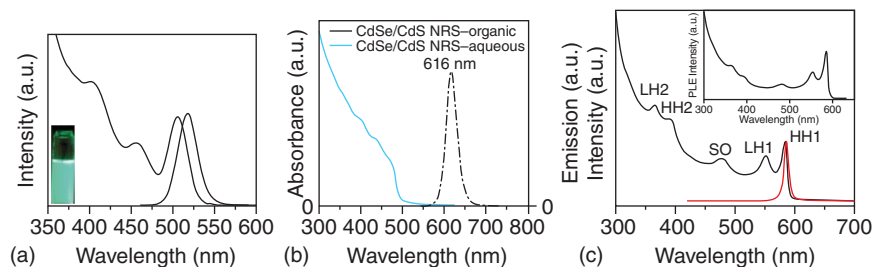


Figure 1.9 Absorption and emission spectra of (a) CdSe/ZnS quantum dots, (b) CdSe/CdS quantum rods, and (c) CdSe quantum sheets.

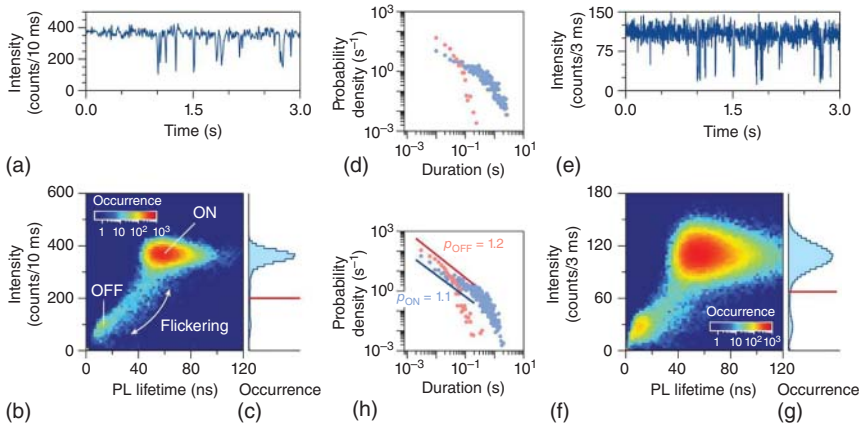


Figure 1.10 (a) Emission intensity from a single CdSe/CdS/ZnS core/shell/shell quantum dot with a temporal resolution of 10 ms under pulsed excitation (405 nm; 10 MHz; $1 \mu\text{m}^2$). The diameter of the quantum dot core is 3.2 nm and the shell has 8(2) CdS(ZnS) monolayers. (b) The corresponding “fluorescence lifetime intensity distribution” is a two-dimensional histogram. The plot is based on a 300 seconds experiment, which was divided into 30 000 10 ms time intervals. The effect of scintillation is highlighted. (c) Corresponding 1D intensity histogram with thresholds used for statistical analysis indicated by red lines. (d) Flicker periods (blue) and non-flicker periods (red) extracted from the 10 ms merged and thresholded data in (a) plot. (e–h) Same as (a–d), but using the same single photon data on which there are 3 ms time bins for statistics. Source: Rabouw et al. [22]/American Chemical Society.

potentially limits QDs from being a stable photoluminescent output source under relatively high fluxes. A different approach to blinking suppression was explored by growing a thick CdS or CdS/CdZnS/ZnS shell (>5 nm in shell thickness) onto CdSe core QDs with the idea of fully isolating the excited carriers from the QD surface and the surface environment [22]. However, these QDs generally do not have a very good size distribution, exhibit broad PL spectra, and display moderate PL QYs. More recently, synthesis of CdSe/CdS QDs at a high reaction temperature (310°C) using octanethiol as a sulfur precursor resolved many of these issues (Figure 1.10).

The terms Type I and Type II QDs are used to classify QDs based on their band structure and electron–hole recombination dynamics (Figure 1.11). Type I and Type

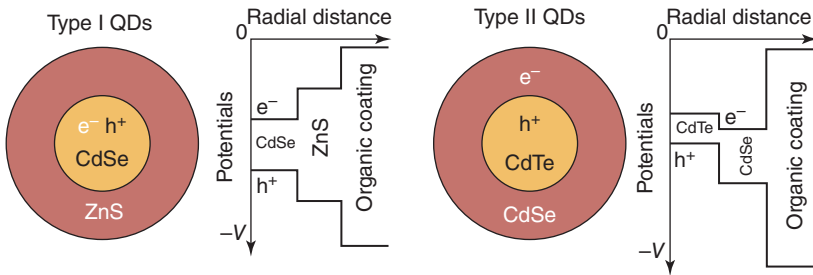


Figure 1.11 Comparison of Type I and Type II CdSe/ZnS core–shell quantum dots. Source: Vaneski [23]/Aleksandar Vaneski.

II QD materials are two different categories of semiconductor nanostructures that exhibit unique electronic and optical properties due to their quantum confinement effects. In a Type I QD, the electrons and holes are confined in the same region of the QD, resulting in a strong overlap of their wave functions. This leads to efficient radiative recombination of the electron–hole pairs, resulting in a high quantum yield and bright fluorescence. Examples of Type I QDs include CdSe, CdTe, and InP QDs. In contrast, in a Type II QD, the electrons and holes are spatially separated between two different regions of the QD due to a band offset at the interface. As a result, radiative recombination of the electron–hole pairs is less efficient than in a Type I QD, leading to lower quantum yields and longer-lived excitons. However, Type II QDs exhibit unique properties such as multiple exciton generation and efficient charge separation, which make them attractive for applications such as solar cells and photocatalysis. Examples of Type II QDs include CdS/CdTe, CdSe/CdTe, and CdSe/ZnTe QDs. Both Type I and Type II QDs have found numerous applications in areas such as optoelectronics, bioimaging, and sensing due to their unique properties and tunability.

Giant QDs are a type of QD structure that is characterized by a larger size and a more complex core–shell structure than traditional QDs. While traditional QDs typically have dimensions on the order of a few nanometers, giant QDs can have dimensions up to tens of nanometers. The larger size of giant QDs offers several advantages over traditional QDs. For example, giant QDs have a higher absorption cross-section, which allows them to absorb more light and generate more charge carriers per photon. They also have a higher quantum yield and longer emission lifetime due to reduced surface recombination and enhanced confinement of excitons. Giant QDs can be synthesized using various methods, including the core–shell approach, which involves the growth of a large core particle, followed by the deposition of multiple layers of shell material. The resulting core–shell structure can have a complex morphology, such as a core–shell–shell or a core–shell–shell–shell structure. Applications of giant QDs include bioimaging, sensing, and photovoltaics. In bioimaging, giant QDs can be used as contrast agents due to their bright and stable emission. In sensing, they can be used as probes for detecting biomolecules due to their high sensitivity and specificity. In photovoltaics, giant QDs can be used as absorbers in thin-film solar cells due to their high absorption efficiency and tunable bandgap.

1.2.4 Continuously Graded Core–Shell Structure of QDs (cg-QDs)

For most core/shell QDs, such as giant CdSe/CdS core–shell QDs (denoted CdSe/CdS g-QDs, where the small CdSe core is passivated by the large CdS shell) synthesized by the successive ion layer adsorption and reaction (SILAR) method, exhibit reduced surface trapping and AR. Notably, this core/shell QD shows a significant redshift of the emission peak, which indicates that the CdSe core wave function extends into the CdS shell region, i.e. the effective size of the core increases. In addition, the first absorption peaks of CdSe/CdS g-QDs are relatively suppressed, which is due to the fact that the bandgap of CdS is larger than that of CdSe, so the absorption mainly comes from the thick CdS shell. However, due to the large

- poly-[(9,9-bis(3'-(*N,N*-dimethylamino)propyl)-2,7-fluorene)-*alt*-2,7-(9,9-*ioctyl*fluorene)] (PFN) 301
- poly((9,9-dioctylfluorenyl-2,7-diyl)-*alt*-(9-(2-ethylhexyl)carbazole-3,6-diyl)) copolymer 315
- poly(indenofluorene-*co*-triphenylamine) copolymer (PIF-TPA) 312, 313
- polyethoxy polyethyleneimine (PEIE) modified conventional ZnO layers 296
- polymer-mediated QD assembly strategy 197
- polymer-modified ETMs 296
- poly [2-methoxy-5-(2'-ethylxyloxy)-1,4-phenyl vinyl] (MEH-PPV) matrix material 181
- poly(3,4-ethylenedioxythiophene): poly(styrene sulfonate) (PEDOT:PSS) 305
- poly-TPD 146, 156, 157, 211, 215, 304–306
- positive aging effect, in QDLED 272–273
- precursor chemistry 55, 56
- proton NMR 69
- PVK/poly-TPD bilayer 309
- pyridine-treated CdSe nanocrystals, NMR spectra of 71
- q**
- QDiP structure simulation 182
- QDiP system 181, 182
- quantum confinement effect 5, 7, 8, 12, 27, 68, 141, 149, 151, 153, 155
- quantum dot display industry 328
- chain 329
- patent layout
- BOE 347–351, 354
- CSOT 344–347
- Najing Tech 338–344
- Nanoco 335–338
- Nanosys 330–332
- SAMSUNG Group 332–335
- TCL 351–354
- quantum dot-enhanced liquid crystal display (QD-LCD) 143, 327, 329, 330, 351
- quantum dot enhancement film (QDEF) 330, 349, 355
- quantum dot light-emitting diodes (QDLEDs) 18, 259
- advantages 235
- ageing and degradation, QD layer impact 276–277
- aging mechanism 271–277
- anode-interface regulation layer 267
- basic structure of 18–19
- cathode-interface regulation layer 267
- characterization technologies for 278–286
- charge transport mechanism 292–293
- commercialization challenge 19
- common materials for functional layer 262
- with Cs₂CO₃/Al cathode and MoO₃/Alq₃ anode 267
- current density-voltage and luminous intensity-voltage curves 265
- development, history of 22–27
- device structure
- conventional 99, 102
- inverted 102
- and performance 100
- tandem 102
- Type I 98
- Type II 98
- Type III 98
- Type IV 98–99
- efficiency and stability of 291
- efficiency decay mechanism 268–271
- electronic transport layer 265–267
- EQE-current density curves 265
- factors affecting light emission 19
- Auger recombination 19–21
- fluorescence resonance energy transfer 21–22
- surface traps and field emission burst 22
- hole transport layer 263–265

- with InP/ZnSe/ZnS quantum dots 99
 - performance degradation causes of 125
 - performance with WO₃ nanoparticles vs. PEDOT:PSS as anode interface layer 268, 269
 - QD light-emitting layer 261–263
 - stability
 - factors affecting 261–268
 - structure 261
 - types of 235
 - working mechanism 261
 - quantum dots (QDs) 51
 - application on display devices 18–27
 - classification 111
 - with direct white light emission 197–200
 - display technology 327
 - energy spectroscopy 197
 - feature of 10
 - fluorescence quantum yield measurement 79
 - ink 347
 - ligand engineering 92
 - light-emitting characteristics of
 - continuously gradated core-shell structure 12, 14
 - core-shell structure 8–12
 - optical property 4–8
 - particle size and emission color 3
 - materials and their properties 14–17
 - in matrix 181
 - photoluminescent display products 327
 - preparation route of 3
 - QD-OLED 329
 - for white LEDs 188–200
 - quantum dots light-emitting diodes (QDLED)
 - device fabrication process 48
 - operating parameters
 - current efficiency 45
 - luminescence color 45
 - luminous brightness 44
 - luminous efficiency 44
 - luminous lifetime 45–46, 48
 - power efficiency 45
 - quantum efficiency 44–45
 - turn-on voltage 44
 - structure of 41–43
 - working principle of
 - carrier injection 43
 - carrier transport 43
 - exciton formation 43–44
 - radiative recombination of excitons 44
 - quantum optical properties 6, 8
 - quantum size effect 1, 4, 5
 - quantum surface effect 4
 - quantum tunnelling effect 5, 6
- r**
- red QDLEDs
 - ageing of 275
 - alloy core-shell structure 96–97
 - breakthrough technology developments 87, 88
 - challenges 103, 104
 - core-shell structure 94–96
 - device architecture development 97
 - with double-hole transport layer 310
 - external quantum efficiency development 87, 88
 - fluorescence emission range 89
 - materials 88–97
 - PIF-TPA as HTL in 312
 - stability studies of 260
 - structure design and optimization range 90–91
 - surface ligands on 91–94
 - research directions, QDLED degradation and aging 287
 - RGB color space parameters 46
- S**
- SAMSUNG Group 332–335
 - sandwich AC-driven thin film electroluminescent (AC-TFEL) device 239
 - Scherrer's formula 77

- Schottky barrier 39, 40
- scintillation phenomenon of quantum dots 21
- selected area electron diffraction (SAED) technique 77
- self-annihilation of quantum dots 181
- self-assembly methods 369
- self-quenching 21
- semiconductor nanocrystals 1, 51, 57, 188, 332, 335
- Se-ZnSe colloidal quantum dots, UV-Vis absorption spectrum of 69
- shell engineering 114, 118, 130, 134
cadmium-free quantum dots 224–227
- SILAR (sequential ion layer adsorption and reaction), core/shell QD synthesis 63
- silicon nanocrystals 178
- silicon quantum dots 15, 17, 178–179
- single-layer quantum dot light-emitting device 41
- single light-emitting white light devices 188
- SiO₂ QDs in perovskite matrix 181
- slow dropping, core/shell QD synthesis 63
- small-angle X-ray scattering (SAXS) 67, 76–77
- solid-state ligand exchange process 179, 180
- solid-state nuclear magnetic resonance (SSNMR) techniques 71
- solubility of CdSe nanocrystals 66, 93
- solution ligand exchange process 179, 180
- solution NMR spectroscopy 70
- solution-prepared inverted QDLEDs 122
- solution processability 33, 34
of colloidal quantum dots 66
- solution-processed method 48
- solution-processed QDLEDs 25, 27, 48, 200, 314
- solvent-resistant blended HTL 315
- spin-coating process 47, 48
- stability 35–36
- surface-adsorbed H₂S 91
- surface chemistry, of colloidal quantum dots
covalent bond classification method 65–66
entropic ligands 66
- surface dipolar polymers 301
- surface ligand modification 87, 90, 91
- surface passivation 61, 176, 201, 247, 287, 328, 336
- surface states, of quantum dots 36
- t**
- tandem QDLED device structure 102
- tandem WQDLEDs 196
- TCL 351–354
- TC-SP (thermocyclically coupled single precursor), core/shell QD synthesis 63
- ternary I–III–VI₂ chalcopyrite semiconductor QDs 17
- tetradecane 57, 58
- 2,2',7,7'-tetrakis[*N*-naphthalenyl(phenyl)amino]-9,9-spirobifluorene (spiro-2NPB) 309
- TFB-BP polymer synthesis and photocross-linking 314
- thermal spin-coating technique 310
- thick-shell structured Zn_{1-x}Cd_xSe/ZnS core/shell quantum dots 130
- thioglycolic acid (TGA) 90, 332
- three base color quantum dot composite 193–197
- 3D cluster-based bcc single supercrystals 78
- time-resolved fluorescence spectroscopy 68
- time-resolved photoluminescence (TRPL) 278, 287
- top-down method, QD preparation 3
- transient electroluminescence (EL) 278–281
- transient fluorescence spectra 68, 70

- transmission electron microscopy (TEM)
7, 67, 76, 278
- tricolor QDs@Psi powders 197
- tri-*n*-octylphosphine (TOP) 127
- tri-*n*-octylphosphine oxide (TOPO)
solution 54
- trioctylphosphine oxide 56, 90, 339
- tris (4-carbazoyl 9-ylphenyl) amine
(TCTA) 158
- two-dimensional nanocrystals 59, 61
- two-dimensional quantum sheets 2
- type I and type II CdSe/ZnS core-shell
quantum dots 11, 12
- type I core-shell structure 95
- type II core-shell QDs 95
- type II core-shell structure 95
- u**
- ultra HD quantum dot TV sets 51
- ultra-thin 1,3,5-tris(1-phenyl-1*H*-
benzimidazol-2-yl)benzene (TPBi)
interface layer 264
- UV-Vis absorption spectroscopy 66–69
- v**
- vacuum evaporation 132, 165
- valence band 1, 3, 37–39, 62, 95, 120,
158
- V₂O₅/PVK heterojunctions, as hole
transport layers 308
- w**
- white LEDs based on quantum dot
photoluminescence mechanism
188
- white QDLED based on CIS class 222
- white quantum dot light-emitting diodes
(WQDLEDs) 188, 195, 201–203
- wide-angle X-ray scattering (WAXS) 67,
76–77
- x**
- X-ray absorption fine structure (XAFS)
spectroscopy 78–79
- X-ray diffraction (XRD) 77, 278
- X-ray diffractometer 77–78
- X-ray diffractometry 77
- X-ray photoelectron spectroscopy (XPS)
74–75
- y**
- YAG hybrid phosphors, for white
light-emitting diodes 189
- yellow-blue composite white light
quantum dots 189–193
- yellow-green emitting CuInS₂ colloidal
quantum dots 190
- z**
- ZCGS/ZnS core-shell quantum dots 222
- zero-dimensional-quantum dots 2
- Zn_{0.95}Mg_{0.05}O as electron transport layer
material 295
- ZnO as ETM 293
- ZnO ETLs fabrication, n-type dopants for
295
- Zn(OA)₂-QDs based IJP QDLED 368
- ZnSe/CdSe/ZnS core-bilayer shell QDs
114
- ZnSe quantum dots 215, 217–218
- ZnSe/ZnS-based blue QDLEDs 215
- ZnS QDs/CBP/MoO₃/Al inverted device
124
- ZnS QDs/CBP/MoO₃/Al QDLED 113
- ZnS quantum dots with 1-octanethiol
ligands 121
- Zn_xCd_{1-x}Se alloyed quantum dots 121
- Zn_{1-x}Cd_xSe/Zn core/shell quantum dots
126
- Zn_{1-x}Cd_xSe/ZnSe/ZnSe_xS_{1-x}/ZnS
core/multi-shell QDs 113